

# CHEVRON CRACK PREDICTION USING THE EXTREMELY LOW STRESS TRIAXIALITY TEST

FRANTISEK SEBEK, PETR KUBIK, JINDRICH PETRUSKA

Brno University of Technology, Institute of Solid Mechanics  
Mechatronics and Biomechanics, Faculty of Mechanical Engineering  
Brno, Czech Republic

DOI: 10.17973/MMSJ.2015\_06\_201518

e-mail: sebek@fme.vutbr.cz

Forward extrusion is typical way of mass-production of cold formed bars or rods with constant cross section. This process is used for production of engine alternator shafts and it is based on reducing the diameter of semi-product without removing material in several reductions. However, there is a potential danger of the chevron cracking. Chevron cracks are inside the material and therefore invisible on the surface of the semi-product. Using computational methods, the potential cracking can be predicted in advance, therefore it may lead to considerable savings. Three various phenomenological ductile fracture criteria were calibrated and then applied to forward extrusion process. As there are specific stress states in this process, new extremely low stress triaxiality fracture test were designed and used in the criteria calibration process. The test is based on the compression of the cylinder with a specific recess.

Then, the criteria prediction ability and reliability is discussed.

## KEYWORDS

forward extrusion, ductile fracture, extremely low stress triaxiality, explicit finite element method, AISI 1045

## 1. INTRODUCTION

The ductile fracture regards ductile polycrystalline metals which can experience large plastic deformations. These irreversible deformations can easily go into hundreds of percent. There are several approaches to ductile fracture, from phenomenological criteria [Cockcroft 1968], across continuum damage mechanics [Lemaitre 1985], and void nucleation, growth and coalescence [Rice 1969] to porosity based models [Gurson 1977]. In scope of phenomenological criteria covered in this paper, the prediction of ductile cracking is based on evaluating the damage related to plastic deformation. This had been originally formulated as hydrostatic pressure dependent [McClintock 1968], but it was shown that there is also the deviatoric stress dependence [Wierzbicki 2005b].

The ductile fracture prediction has a broad potential. It can cover various engineering applications, such as machining [Umer 2014], leveling [Petruska 2012], or high velocity impacts [Teng 2004].

The forward extrusion of cylindrical semi-products is based on reduction of the diameter [Petruska 2013], in our case in six consequential reductions. Critical is the abrupt change of stress state at the axis of symmetry when material leaves the conical process zone of the extrusion die. Due to combined effect of friction and drop of normal contact stress, hydrostatic compression is reversed to tension. The friction plays crucial role in the process. Rule that the less friction there is the better the process goes does not apply. With excessive amount of lubrication, the material nearby the surface flows faster than the rest close to the axis and the risk of cracking is increased. Chevron cracks are result of repetitive tensile stresses related to heterogeneous deformation in central part of the semi-product. The danger of chevron cracks arises from their invisibility on the surface of the semi-product. One non-destructive way how to inspect the internal cracks is to use of the X-ray.

There were selected three phenomenological ductile fracture criteria, model proposed by Bai and Wierzbicki [Bai 2008], Extended Mohr-Coulomb criterion [Bai 2010], and model proposed by Lou et al. [Lou 2014]. The first above model does not have a cut-off value compared to others. All the models have the asymmetric weighting function of damage with respect to normalized Lode angle. Mentioned criteria differ especially in the number of material constants which have to be calibrated from fracture tests. To calibrate these models reliably, various stress states should be described by the tests. Then, calibrated models can be used for solids subjected to multi-axial loading. It should be noted that there cannot be numerical computation without the experimentation, these two go hand in hand.

## 2. EXPERIMENTS

AISI 1045 carbon steel, used in automotive industry or as a common structural steel, was a subject of examination.

### 2.1 PLASTICITY

Classical von Mises plasticity with isotropic hardening was used. To obtain material work hardening, tensile tests of smooth cylindrical specimen with 6 mm in diameter (Fig. 1) were carried out. Experimentally obtained force-displacement response was used to calculate the engineering stress-strain curve which served to estimate the true, or also equivalent in the case of uniaxial tension, stress-strain curve up to the ultimate tensile strength. Then, the true curve served as an input to the trial and error method when the computational simulation of tensile test was carried out in order to extrapolate the curve beyond the ultimate tensile strength.



Figure 1. Geometries of cylindrical and notched tube specimens

The final multi-linear flow curve, the equivalent stress-strain curve depicted in Fig. 3, was obtained when satisfying match between force-displacement curve from experiment and computation had been reached (Fig. 2).

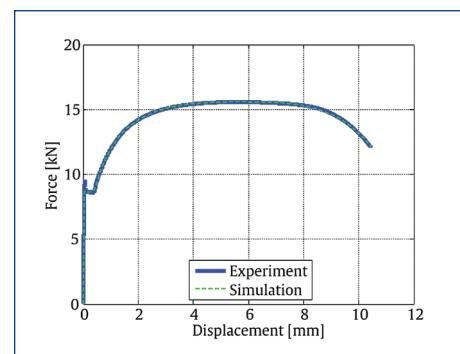


Figure 2. Force-displacement curves from experiment and computation

As there are two plasticity related material constants needed in Extended Mohr–Coulomb criterion [Bai 2010], the Hollomon hardening law in Eq. (1) [Hollomon 1945] was fitted to multi-linear flow curve. The equivalent stress is

$$\bar{\sigma} = K\bar{\varepsilon}^n \quad (1)$$

where  $K$  is the strength coefficient,  $\bar{\varepsilon}$  is the equivalent strain, and  $n$  is the strain hardening exponent.

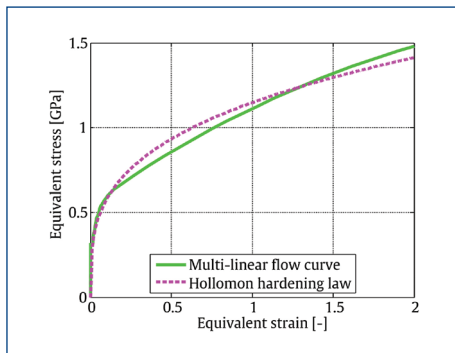


Figure 3. Multi-linear flow curve and the one fitted by Hollomon hardening law

The multi-linear flow curve was then used in all subsequent computational simulations.

## 2.2 FRACTURE

In order to calibrate selected fracture criteria, additional fracture tests were carried out. Besides tensile test of smooth round specimen, there were conducted tensile tests of notched round specimens, biaxial tests of notched tube specimens and compression of cylinder with specific recess.

The gauge length in case of smooth cylindrical specimen as well as notched cylindrical specimens was 30 mm. The smallest diameter of notched cylindrical specimens was 6 mm, the same as in case of smooth cylindrical specimen. Notch radii were R1.2, R2.5, and R5. Force-displacement curves from experiments and computations for each radius of notched cylindrical specimens (Fig. 1) are depicted in Fig. 4.

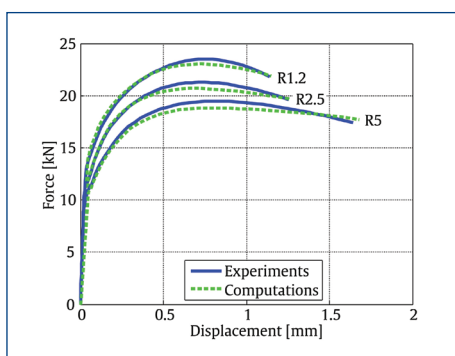


Figure 4. Force-displacement curves from experiments and computational simulations for notched cylindrical specimens

Notched tube had R3 notch radius with 9 mm in diameter in the smallest region of the notch (Fig. 1). The inner diameter of the tube was 7 mm. Biaxial tests of notched tube specimens generated different stress states by different combination of tension or compression and torsion. The loading combination  $R$  can be expressed as the ratio of axial  $u$  to torsional  $\omega$  movements, respectively.

$$R = \frac{u}{\omega} \quad (2)$$

In order to cover the largest region of plane stress in the plane of stress triaxiality and normalized Lode angle (Fig. 11), following loading ratios were selected,  $-1, -0.5, 0, 0.5, 1, 4.2,$  and  $\text{inf}$  mm/rad. Force-displacement and torque-rotation curves from experiments and computations for notched tube specimens are depicted in Figs. 5 and 6, respectively.

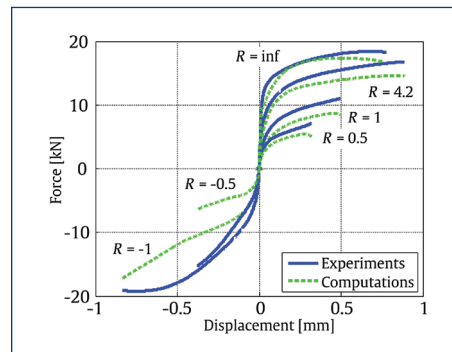


Figure 5. Force-displacement curves from experiments and computational simulations, respectively, for notched tube specimens

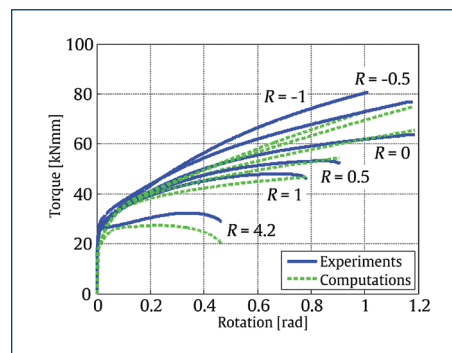


Figure 6. Torque-rotation curves from experiments and computational simulations, respectively, for notched tube specimens

Last of the fracture tests used for ductile fracture criteria calibration was the compression of cylinder with spherical recess. This novel specimen was designed so as to reach extremely low stress triaxiality. Geometry of the cylinder is depicted together with force-displacement curves from experiment and computational simulation in Fig. 7.

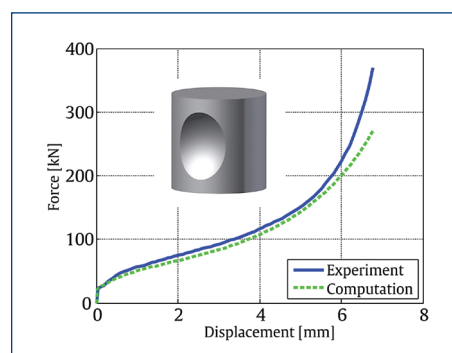


Figure 7. Force-displacement curves from experiment and computation for depicted compressed cylinder with spherical recess

## 2.3 FORWARD EXTRUSION

The paper aims to show the reliability and prediction capability of selected fracture criteria calibrated using, among others, extremely low stress triaxiality test designed to approach the stress state near to the one reached in forward extrusion of cylindrical rod. In the beginning

of the process, the semi-product has 27 mm in diameter and 22 mm in length. Then, the cylindrical rod is reduced to 13.2 mm in diameter in six subsequent reductions. The X-ray revealed that there were no internal defects after the fifth reduction (Fig. 8) and there were chevron cracks after the sixth one (Fig. 9).



Figure 8. The X-ray of semi-products after the fifth reduction without chevron cracks

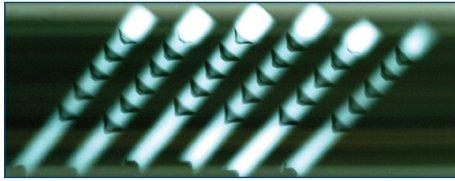


Figure 9. The X-ray of semi-products after the sixth reduction with chevron cracks

The axial cut of cylindrical rod after the experiment when six reductions were completed is depicted in Fig. 10. Cracks were initiated in the centre of the rod by void nucleation, growth and coalescence and then propagated by the shear mechanism to form conical chevron shape.

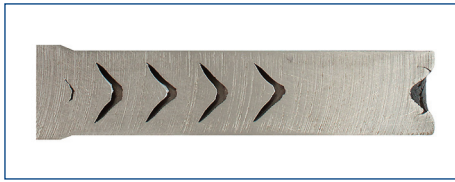


Figure 10. Axial cut of the cylindrical rod after the experiment with chevron cracks

### 3. CRITERIA CALIBRATION

In order to reliably calibrate phenomenological criteria, it is important to cover the space of stress states (Fig. 11), represented by the plane of stress triaxiality given in Eq. (3) and normalized Lode angle given in Eq. (4), by independent experiments as much as possible. It is often convenient to use universal specimens in terms of reaching different stress states by changing loading conditions. Widespread universal specimen is the so-called butterfly specimen [Wierzbicki 2005a] or notched tube specimen (Fig. 1).

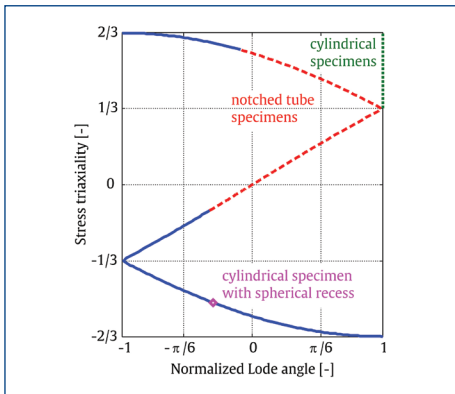


Figure 11. Plane of stress triaxiality and normalized Lode angle with highlighted regions covered by realized experiments

Using the mean and equivalent stresses,  $\sigma_m$  and  $\bar{\sigma}$ , respectively, the stress triaxiality is expressed as

$$\eta = \frac{\sigma_m}{\bar{\sigma}} \quad (3)$$

Normalized Lode angle is using the deviatoric stress tensor  $S$  defined as follows

$$\bar{\theta} = 1 - \frac{2}{\pi} \arccos\left(\frac{27 \det(S)}{2 \bar{\sigma}^3}\right) \quad (4)$$

The crucial part of any phenomenological ductile fracture criteria is its so-called weighting function of damage  $\bar{\epsilon}_f(\eta, \bar{\theta})$ , which can also contain the cut-off, dependent both on the stress triaxiality and normalized Lode angle. The cut-off value represents the region with no fracture or the boundary in Fig. 11 below the do not occur. In the beginnings, it was believed that the fracture does not occur under the stress triaxiality of value  $-1/3$  which had to be incorporated in the particular weighting function of damage. Using this weighting function, the damage can be incrementally accumulated through the plastic strain  $\bar{\epsilon}_p$  as

$$D = \int_0^{\bar{\epsilon}_p} \frac{1}{\bar{\epsilon}_f(\eta, \bar{\theta})} d\bar{\epsilon}_p \quad (5)$$

The damage parameter ranges from 0 to 1, while 1 is a critical value when fracture occurs. The loading path is tracked through the cumulative plastic strain  $\bar{\epsilon}_D$ .

Numerical simulations of fracture tests had to be conducted prior to criteria calibration in order to obtain variables which cannot be experimentally obtained. Those are the fracture strain, average stress triaxiality and normalized Lode angle.

The weighting function of damage of model proposed by Bai and Wierzbicki [Bai 2008] with no cut-off value is

$$\bar{\epsilon}_f(\eta, \bar{\theta}) = \left[ \frac{1}{2} (D_1 e^{-D_2 \eta} + D_2 e^{-D_3 \eta}) - D_3 e^{-D_4 \eta} \right] \bar{\theta}^2 + \frac{1}{2} (D_1 e^{-D_2 \eta} - D_2 e^{-D_3 \eta}) \bar{\theta} + D_3 e^{-D_4 \eta} \quad (6)$$

The model has six material constants  $D_1, \dots, D_6$ , sequentially 2.3890, 1.6398, 1.1983, 0.7981, 1.1810, and 1.3529 which were calibrated using the non-linear least square method in the software MATLAB using the values obtained from numerical simulations of fracture tests. These constants were used in designing the fracture envelope of the model in Fig. 12.

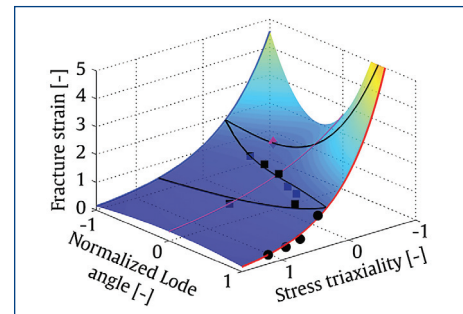


Figure 12. Fracture envelope of model proposed by Bai and Wierzbicki

There is apparent the pressure dependence in Fig. 12 where the fracture strain increases with decreasing stress triaxiality. The so-called Lode dependence is also obvious. The fracture strain is decreasing when moving from axisymmetric tension or compression,  $\bar{\theta} = 1$ , or  $\bar{\theta} = -1$ , respectively, to plane strain or generalized shear,  $\bar{\theta} = 0$ .

Extended Mohr–Coulomb criterion [Bai 2010] has a weighting function of damage, with gradual cut-off, defined as

$$\bar{\epsilon}_f(\eta, \bar{\theta}) = \left\{ \frac{K}{E_2} \left[ \sqrt{\frac{1+E_1^2}{3}} \cos\left(\frac{\pi}{6} \bar{\theta}\right) + E_1 \left[ \eta + \frac{1}{3} \sin\left(\frac{\pi}{6} \bar{\theta}\right) \right] \right] \right\}^{\frac{1}{n}} \quad (7)$$

With the same procedure as before, two material constants  $E_1$  and  $E_2$  were evaluated as 0.1176 and 668.35 MPa, along with plasticity related constants, the strain hardening exponent and strength coefficient, 0.2998 and 1147.6 MPa, respectively. The fracture envelope is for calibrated constants depicted in Fig. 13.

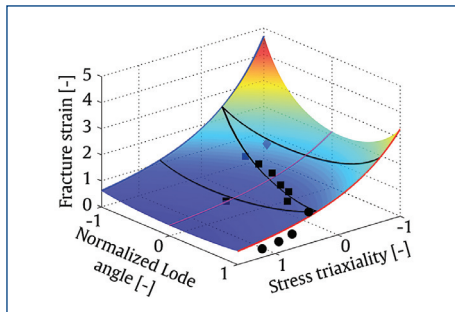


Figure 13. Fracture envelope of Extended Mohr–Coulomb criterion

The weighting function of damage of model proposed by Lou *et al.* [Lou 2014] with three material constants is following

$$\bar{\varepsilon}(\eta, \bar{\theta}) = L_s \left( \frac{2}{\sqrt{3} \left[ 1 + \tan^2 \left( -\frac{\pi}{6} \bar{\theta} \right) \right] \right)^{-L_1} \left( \frac{1}{1+L} \right) \left( \eta + \frac{3 - \sqrt{3} \tan \left( -\frac{\pi}{6} \bar{\theta} \right)}{\sqrt{27 \left[ 1 + \tan^2 \left( -\frac{\pi}{6} \bar{\theta} \right) \right]} + L} \right)^{-L_2} \quad (8)$$

The angle brackets  $\langle \rangle$  denote the Macaulay bracket notation. Material constant  $L$  representing the cut-off value sensitivity has to be carefully chosen and fixed before the calibration process. In this case, it was at value of 1/3. Additional material constants  $L_1, \dots, L_3$ , are sequentially -2.0223, 0.3525, and 0.7727. The fracture envelope is depicted in Fig. 14 where there is a noticeable sudden cut-off as well.

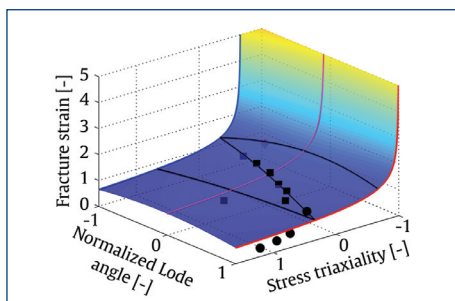


Figure 14. Fracture envelope of model proposed by Lou *et al.* with a sudden cut-off

#### 4. COMPUTATIONS AND RESULTS

After the fracture criteria had been calibrated, the computational simulation of forward extrusion with chevron cracking could be performed. The subroutine VUMAT within the Abaqus/Explicit FEM commercial package was used.

Six reductions with semi-cone reductions had 20° were realized. Phosphate was applied on surface of the rod after each reduction to reduce friction, therefore 0.1 friction coefficient was considered. No friction is supposed behind the conical reduction where the material enters the open space.

There is more methods how to predict the ductile crack initiation and propagation. The element deletion technique, which is easy to implement, was used in the present paper. The disadvantage of the method is the losing of mass, so affected elements should have small dimensions not causing any misbalance in computations.

The problem was modelled as axisymmetric with bilinear quadrilateral CAX4R finite elements with reduced integration and characteristic size 0.075 mm in the process region of the semi-product.

There are fields of damage parameter for each criterion in Fig. 15 with unified legend scale from 0 to 1. The cracking correctly occurred in the sixth reduction in case of model proposed by Bai and Wierzbicki. The cracking was predicted wrongly in the fifth reduction when the Extended Mohr–Coulomb criterion was used and finally, the cracks occurred wrongly in the fourth reduction in case of model proposed by Lou *et al.*

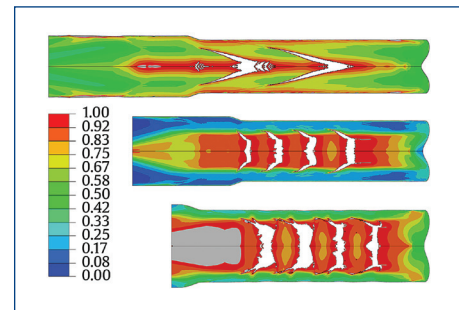


Figure 15. Fields of damage parameter plotted on rods for model proposed by Bai and Wierzbicki (top), Extended Mohr–Coulomb criterion (middle), and model proposed by Lou *et al.* (bottom)

The point on the axis of symmetry 14 mm from the left face of the original semi-product was taken for analysis of damage evolution during the computational simulation using model proposed by Bai and Wierzbicki. It is obvious that the damage accumulated almost solely when the normalized Lode angle equalled unity (Fig. 16). Therefore, the formation of chevron cracks is influenced by the fracture strain under the condition of symmetric tension.

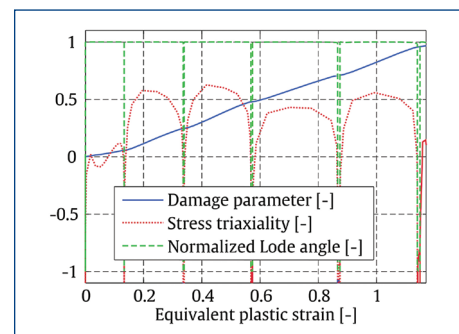


Figure 16. The damage evolution during computational simulation using model proposed by Bai and Wierzbicki

#### 5. CONCLUSIONS

Forward extrusion of cylindrical rods of AISI 1045 carbon steel were examined. The novel specimen was designed to describe extremely low stress triaxiality where the process region of forward extrusion is really situated. Three phenomenological ductile fracture criteria were selected and calibrated using the novel specimen and cylindrical and notched tube specimens as well. Then, they were applied to the extrusion cold working process. Results revealed that the model proposed by Bai and Wierzbicki predicted correctly the onset of cracking in the sixth reduction but with wrong number and shape of cracks. The Extended Mohr–Coulomb criterion predicted the cracking wrongly in the fifth reduction but with correct number and shape of cracks. And finally, the model proposed by Lou *et al.* predicted the onset of cracking wrongly in the fourth reduction, two reductions earlier than in the experiment, and with wrong number and shape of cracks. Moreover, there was non-negligible loss of volume in this case which is not realistic. Better results could probably be obtained using some criterion combining features of the model proposed by Bai and Wierzbicki and Extended Mohr–Coulomb criterion. The role of friction is one of challenging features to study in the future.

## ACKNOWLEDGMENT

This work is an output of project NETME CENTRE PLUS (LO1202) created with financial support from the Ministry of Education, Youth and Sports under the „National Sustainability Programme I“.

## REFERENCES

- [Bai 2008] Bai, Y. and Wierzbicki, T. A new model of metal plasticity and fracture with pressure and Lode dependence. *International Journal of Plasticity*, June 2008, Vol. 24, pp 1071-1096, ISSN 0749-6419, DOI: 10.1016/j.ijplas.2007.09.004.
- [Bai 2010] Bai, Y. and Wierzbicki, T. Application of extended Mohr-Coulomb criterion to ductile fracture. *International Journal of Fracture*, January 2010, Vol. 161, Issue 1, pp 1-20, ISSN 0376-9429, DOI: 10.1007/s10704-009-9422-8.
- [Cockroft 1968] Cockcroft, M.G. and Latham, D.J. Ductility and the Workability of Metals. *Journal of the Institute of Metals*, 1968, Vol. 96, pp 33-39.
- [Gurson 1977] Gurson, A.L. Continuum Theory of Ductile Rupture by Void Nucleation and Growth: Part I–Yield Criteria and Flow Rules for Porous Ductile Media. *Journal of Engineering Materials and Technology*, January 1977, Vol. 99, No. 1, pp 2-15, ISSN 0094-4289, DOI: 10.1115/1.3443401.
- [Hollomon 1945] Hollomon, J. H. Tensile deformation. *Metals Technology*, June 1945, pp 268-290, ISSN 0096-5855.
- [Lemaitre 1985] Lemaitre, J. A continuous damage mechanics model for ductile fracture. *Journal of Engineering Materials and Technology*, January 1985, Vol. 107, No. 1, pp 83-89, ISSN 0094-4289, DOI: 10.1115/1.3225775.
- [Lou 2014] Lou, Y., et al. Modelling of shear ductile fracture considering a changeable cut-off value for stress triaxiality. *International Journal of Plasticity*, March 2014, Vol. 54, pp 56-80, ISSN 0749-6419, DOI: 10.1016/j.ijplas.2013.08.006.
- [McClintock 1968] McClintock, F.A. A Criterion for Ductile Fracture by the Growth of Holes. *Journal of Applied Mechanics*, June 1968, Vol. 35, No. 2, pp 363-371, ISSN 0021-8936, DOI: 10.1115/1.3601204.
- [Petruska 2013] Petruska, J., et al. Ductile Fracture Criteria in Prediction of Chevron Cracks. *Advanced Materials Research*, April 2013, Vol. 716,

pp 653-658, ISSN 1022-6680, DOI:10.4028/www.scientific.net/AMR.716.653.

[Petruska 2012] Petruska, J., et al. A New Model for Fast Analysis of Leveling Process. *Advanced Materials Research*, October 2012, Vol. 586, pp 389-393, ISSN 1022-6680, DOI:10.4028/www.scientific.net/AMR.586.389.

[Rice 1969] Rice, J.R. and Tracey, D.M. On the ductile enlargement of voids in triaxial stress fields. *Journal of the Mechanics and Physics of Solids*, June 1969, Vol. 17, Issue 3, pp 201-217, ISSN 0022-5096, DOI: 10.1016/0022-5096(69)90033-7.

[Teng 2004] Teng, X. and Wierzbicki, T. Effect of fracture criteria on high velocity perforation of thin beams. *International Journal of Computational Methods*, June 2004, Vol. 01, Issue 01, pp 171-200, ISSN 0219-8762, DOI: 10.1142/S0219876204000058.

[Umer 2014] Umer, U., et al. Finite element modeling of the orthogonal machining of particle reinforced aluminum based metal matrix composites. *MM Science Journal*, December 2014, pp 511-515, ISSN 1803-1269, DOI: 10.17973/MMSJ.2014\_12\_201416.

[Wierzbicki 2005a] Wierzbicki, T., et al. A new experimental technique for constructing a fracture envelope of metals under multi-axial loading. In: *Proceedings of the 2005 SEM annual conference and exposition on experimental and applied mechanics*, Portland, 7-9 June, 2005, pp 1295-1303.

[Wierzbicki 2005b] Wierzbicki, T., et al. Calibration and evaluation of seven fracture models. *International Journal of Mechanical Sciences*, April-May 2005, Vol. 47, Issues 4-5, pp 719-743, ISSN 0020-7403, DOI: 10.1016/j.ijmecsci.2005.03.003.

## CONTACTS

Ing. Frantisek Sebek, Ing. Petr Kubik, prof. Ing. Jindrich Petruska, CSc.  
Institute of Solid Mechanics, Mechatronics and Biomechanics  
Faculty of Mechanical Engineering, Brno University of Technology  
Technicka 2896/2, Brno, 616 69, Czech Republic  
tel.: +420 54114 4925, +420 54114 2858,  
e-mail: sebek@fme.vutbr.cz, ykubik05@stud.fme.vutbr.cz,  
petruska@fme.vutbr.cz  
www.umt.fme.vutbr.cz/cz/